



Chen, J., Wang, Y., & Jia, B., et al. (2011). Observation of the inverse Doppler effect in negative-index materials at optical frequencies.

Originally published in *Nature Photonics*, 5(4), 239–245.
Available from: <http://dx.doi.org/10.1038/nphoton.2011.17>

Copyright © Macmillan Publishers Limited.
The original publication is available at <http://www.nature.com/>.

This is the author's version of the work. It is posted here with the permission of the publisher for your personal use. No further distribution is permitted. If your library has a subscription to this journal, you may also be able to access the published version via the library catalogue.



Observation of the inverse Doppler effect in negative-index materials at optical frequencies

Jiabi Chen¹, Yan Wang^{1,2}, Baohua Jia³, Tao Geng^{1*}, Xiangping Li³, Lie Feng¹,
Wei Qian¹, Bingming Liang¹, Xuanxiong Zhang¹, Min Gu^{3*}, and Songlin Zhuang¹

¹Shanghai Key Lab of Contemporary Optical System, Optical Electronic Information and
Computer Engineering College, University of Shanghai for Science and Technology,
Shanghai 200093 China

²College of physics and communication electronics, Jiangxi Normal University,
Nanchang 330022 China

³Center for Micro-Photonics and CUDOS, Swinburne University of Technology,
John Street Hawthorn, Victoria 3122, Australia

*Corresponding author: max_geng@yahoo.com.cn and mgu@swin.edu.au

The Doppler effect is a fundamental frequency shift phenomenon that occurs whenever a wave source and an observer are moving with respect to each other. It has well-established applications in astrophotonics, biological diagnostics, weather and aircraft radar systems, velocimeter and vibrometry. The counterintuitive inverse Doppler effect was theoretically predicated in 1968 by Veselago ¹ in the so-called negative-index material (NIM) ². However, because of the tremendous challenges of

frequency shift measurements inside the NIM, most investigations of the inverse Doppler effect have been limited to theoretical predications and numerical simulations³⁻⁷. Indirect experimental measurements have been conducted only in nonlinear transmission lines at 1~2 GHz⁸ and in acoustic media at 1-3 KHz⁹. Here, we report on the first experimental observation of the inverse Doppler shift at the optical frequency ($\lambda=10.6 \mu\text{m}$) by refracting a laser beam in a photonic crystal (PC) prism, which has the NIM property.

Our common experience with the Doppler shift (Δf_D), coming from a passing vehicle for example, is when the source approaches the observer, the detected frequency (f') is higher than the source frequency (f_0) (Fig. 1a). Vice versus, signal with lower frequency is detected when the wave source is moving away. This occurs because the wave propagates in the naturally existing positive refractive index media, where the group velocity \vec{v}_g and the wave vector \vec{k} are parallel, i.e. $\vec{v}_g \cdot \vec{k} > 0$. A fascinating inverse Doppler effect has been predicated in tailored artificial materials², for example a photonic bandgap material which possesses the NIM property ($\vec{v}_g \cdot \vec{k} < 0$). In such NIM materials the electric field \vec{E} , the magnetic field \vec{H} and the wave vector \vec{k} are composed of a set of left-handed coordinates instead of the conventional right-handed coordinates. The phase velocity of light wave propagates in the opposite direction of the energy flow leading to the subversion of fundamental physical rules and intriguing phenomena², including the backward wave propagation, reversed Cerenkov radiation and the inverse Doppler effect, as depicted in Fig. 1b, in which a red-shifted signal is detected for a wave source approaching the detector.

Experimental observation of such an inverse Doppler effect in the optical region is of

great challenge because the frequency is too high to be measured directly. The Doppler shift is usually detected using heterodyne interferometry. However, with the normal heterodyne interferometry, even if the inverse Doppler effect has occurred, it cannot be identified by recording the Doppler shifts simply because the recorded Doppler shifts $\Delta f_D = |f' - f_0|$ are absolute values, which are identical for waves propagating in a positive medium or in a negative medium. Therefore, it is critical to find a way to distinguish the normal and anomalous Doppler effects explicitly.

For this purpose, we design a highly sensitive two-channel heterodyne interferometric experimental setup as shown in Fig. 2 to measure the anomalous Doppler effect in a two-dimensional (2D) PC prism showing the NIM property at 10.6 μm . The proposed PC prism consists of a triangular array of Si rods in air (Fig. 3a). The incident light is along the ΓM direction, as shown in the inset of Fig. 3a. The PC has a rhombus geometry with a side of 5 mm and a vertex angle of 60°. The radii of the Si rods are $r = 0.2a$, where $a = 5 \mu\text{m}$ is the lattice constant and the height of the Si rods is $d = 50 \mu\text{m}$.

The band diagram calculated with a plane wave method¹⁰ for an ideal 2D PC (symmetric dielectric pillars with an infinite height) of the same geometry reveals that complete bandgaps exist between the 1st and 2nd band and the 3rd and 4th band for the TM polarized (with the E field parallel to the Si rods) incident beam, as shown in Fig. 3b. The equifrequency surface (EFS) contours in the \vec{k} space of the PC at several relevant frequencies in the 2nd band are shown in Fig. 3c, where the EFS contour shrinks when the frequency increases clearly indicating that the region in the 2nd band, extending from $f = 0.436$ ($\lambda = 11.47 \mu\text{m}$) to $f = 0.542$ ($\lambda = 9.23 \mu\text{m}$), having $\vec{v}_g \cdot \vec{k} < 0$, is of particular interest^{11,12}. The

fact that the EFS in the first Brillouin zone is almost spherical suggests that the PC is a strongly modulate PC¹¹ thus the light propagation angle can be simply derived from the Snell's law (see Supporting Information). The effective phase index n_p ¹³ for the 2nd band along the ΓM direction is presented in Fig. 3d. At the investigated frequency $f = 0.4717$ ($\lambda = 10.6\mu m$) n_p is approximately -0.7 .

Transmission measurements are performed to verify the negative refraction of the PC prism. As shown in Fig. 2, a TM polarized beam from a CO₂ laser at the desired wavelength ($\lambda = 10.6\mu m$) is incident along the ΓM direction to the PC interface. To ensure most of the energy of the beam ($\sim 3-4$ mm) propagates through the PC prism (50 μm in height), we use a ZnSe lens with a focal distance of 50 mm and a convergence angle of 4° to focus the incident beam into the sample. Both the PC prism and the detector are placed on computer controlled rotation and translation stages to allow individual positioning and angle adjustment. The detector is rotated around the rotation center O to record the intensity of the refracted beam at all rotation angles θ , as shown in Fig. 4a inset, so that the desired negative refractive angle can be found.

The experimental result is presented in Fig. 4a. At a refraction angle of approximately $\theta = -26^\circ$ (incident angle is 60°) high intensity signal could be measured clearly indicating that the PC prism is operating in the negative refraction region, with a measured $n_p = -0.5062$. The result is reproducible for different samples of the same geometry with a $\pm 4^\circ$ error range of the refraction angle. The measured n_p is slightly smaller than the theoretical estimation (-0.7) mainly due to the finite height of the 2D PC in the experiment, which is different from the infinite height of rods assumed in the calculation¹⁴⁻¹⁶ (see Supporting Information).

To measure the Doppler effect the same setup in Fig. 2 is employed. The PC prism is fixed at the measured negative refraction angle and the translation stage is moving uniformly along the x-axis to generate a relative velocity with respect to the detector setting to be perpendicular to the beam propagating direction. During the experiment, the CO₂ laser and the detector are both static. In order to distinguish the normal and anomalous Doppler effect a reference beam is employed in the system. The beam splitter 2, which is placed on the same translation stage as that of the PC prism, as depicted in the inset of Fig. 3, is used to parallel combine the reference beam and the signal beam refracted by the PC prism.

Considering the velocity of the translation stage is along the +x-axis (see Supporting Information for -x-axis displacement), the schematic diagram of light propagating in the PC prism is shown in Fig. 2. Since the propagating direction of the CO₂ laser beam is perpendicular to the incident interface of the prism, the interface velocity in the direction of light propagation is zero. Therefore, no Doppler shift occurs at this incident interface. For the exit interface of the prism, the velocity in the direction of light propagation can be written as $v_1 = v \cot(\pi/6)$, where v is the velocity of the translation stage. Therefore, the Doppler frequency shift at the second interface can be calculated simply:

$$f_1 = f_0 \left(1 - \frac{v_1}{c} n_p\right) = f_0 \left(1 - \frac{v \cot(\pi/6)}{c} n_p\right) \quad , \quad (1)$$

where f_0 is the original frequency of the CO₂ laser, and c is the light velocity in vacuum.

When n_p is negative, f_1 is larger than f_0 , and thus the inverse Doppler effect occurs.

By taking the relative movement between the PC prism and the detector into consideration, the exit interface of the prism, which can be considered as an effective source of the outgoing light, moves towards the detector. Since the transmitting medium is air with a

positive index of unity, the second Doppler effect is normal. Therefore, the recorded Doppler frequency shift at the detector surface can be calculated as

$$f_2 = f_1 \left(\frac{c}{c - v_2} \right) = f_1 \left(\frac{c}{c - v \cot(\pi/6) \cdot \cos(\pi/3 + \theta)} \right) = f_1 k \quad , \quad (2)$$

where a new parameter k is defined as $k = \frac{c}{c - v \cot(\pi/6) \cdot \cos(\pi/3 + \theta)}$ which is always positive and close to 1 in the non-relativistic regime, i.e. $v \ll c$.

For the reference beam, since the beam splitter 2 is mounted on the same translation stage as the PC prism, it posses the same displacement along the x-axis. The velocity of the beam splitter 2 in the beam incident direction can be written as $v_1' = \frac{\sin(2\pi/3 - \beta/2 - \theta)}{\sin(\pi/2 - \beta/2)} v$,

where β is the angle between the incident beam and the reflected beam, as shown in Fig. 2 inset. Therefore, the first Doppler frequency shift at the beam splitter surface can be calculated as

$$f_1' = f_0 \left(1 + \frac{v_1'}{c} \right) \quad . \quad (3)$$

For the relative movement between the beam splitter 2 and the detector, the beam splitter 2 can also be considered as an effective source of the reflected light and its velocity in the light reflection direction can be written as $v_2' = v_1' \cos \beta$. Therefore, the reference Doppler frequency shift at the detector surface can be calculated as:

$$f_2' = f_1' \left(\frac{c}{c - v_2' \cos \beta} \right) = f_0 \left(1 + \frac{v_1'}{c} \right) \left(\frac{c}{c - v_1' \cos \beta} \right) \quad . \quad (4)$$

The frequency difference between the signal frequency f_2 from the PC prism and the reference frequency f_2' from the beam splitter 2 can be obtained from Eq. 2 and Eq. 4:

$$\Delta f = |f_2' - f_2| = |(f_2' - f_0 k) - (f_1 - f_0) k| \quad . \quad (5)$$

In Eq. 5, the first part $f'_2 - f_0 k$ is independent of the effective phase index n_p and can be calculated easily according to the experimental conditions. Under the experimental condition $\theta = -26^\circ$ and $\beta = 45^\circ$; the calculated values of $f'_2 - f_0 k$ at four experimental velocities $0.0123 \text{ mm}\cdot\text{s}^{-1}$, $0.0245 \text{ mm}\cdot\text{s}^{-1}$, $0.0488 \text{ mm}\cdot\text{s}^{-1}$ and $0.0732 \text{ mm}\cdot\text{s}^{-1}$ are all positive, and equal to 1.90 Hz, 3.77 Hz, 7.51 Hz and 11.27 Hz, respectively, as shown in Fig. 4b (also see Supporting Information). Hence, if the measured beat frequency $\Delta f < f'_2 - f_0 k$, note that $k > 0$, the Doppler shift $\Delta f_D = f_1 - f_0$ can and can only be positive, i.e. $f_1 > f_0$, which indicates that the Doppler frequency is blue-shifted and larger than the original frequency of the CO₂ laser when the optical path becomes larger in the NIM. Thus the anomalous Doppler effect occurring in the NIM PC prism can be explicitly demonstrated.

In Fig. 4b inset, the recorded signals from the detector at the above-mentioned four velocities are presented. The frequency differences Δf can be obtained by the fast Fourier transform (FFT) from the recorded signals, and are equal to 0.89 Hz, 1.83 Hz, 3.65 Hz and 5.14 Hz, respectively, which match well with the theoretically calculated values with a relative error of <5% if a measured negative index n_p is -0.5062 is considered (see Supporting Information). It can be clearly seen that all the measured frequency differences Δf are less than $f'_2 - f_0 k$ at the corresponding velocities. This result clearly indicates that the observed Doppler effect is anomalous and thus the inverse Doppler effect has been explicitly observed at the optical frequencies for the first time. The experimental results are reproducible for different PC prisms with the same crystal structure.

To further verify the results and the reliability of our experimental setup, we conduct comparison experiments with a positive-index ZnSe prism ($n_p=2.403$) using the similar

method mentioned above. As expected the measured frequency differences Δf for four velocities are all less than $|f'_2 - f_0 k|$ as shown in Fig. 4c (note that here $f'_2 - f_0 k < 0$), which clearly demonstrates that the Doppler effect measured in the ZnSe prism is normal (see Supporting Information). In addition, the relative errors between the theoretical expectation and the experimental measurement are less than 3% (see Supporting Information), which indicates that the transmission method is as suitable as the reflection method for Doppler shift measurement. Thus the experimental results have demonstrated that our setup can explicitly distinguish the normal and anomalous Doppler effects reliably.

References:

- 1 Veselago, V. G. Electrodynamics of substances with simultaneously negative values of sigma and mu. *Sov. Phys. Usp.* **10**, 509-514 (1968).
- 2 Shalaev, V. M. Optical negative-index metamaterials. *Nat. Photonics* **1**, 41-48 (2007).
- 3 Reed, E. J., Soljacic, M. & Joannopoulos, J. D. Reversed Doppler effect in photonic crystals. *Phys. Rev. Lett.* **91**, 133901 (2003).
- 4 Leong, K., Lai, A. & Itoh, T. Demonstration of reverse Doppler effect using a left-handed transmission line. *Microw. Opt. Technol. Lett.* **48**, 545-547 (2006).
- 5 Kozyrev, A. B. & van der Weide, D. W. Explanation of the inverse Doppler effect observed in nonlinear transmission lines. *Phys. Rev. Lett.* **94**, 203902 (2005).
- 6 Luo, C. Y., Ibanescu, M., Reed, E. J., Johnson, S. G. & Joannopoulos, J. D. Doppler radiation emitted by an oscillating dipole moving inside a photonic band-gap crystal. *Phys. Rev. Lett.* **96**, 043903 (2006).
- 7 Kats, A. V., Savel'ev, S., Yampol'skii, V. A. & Nori, F. Left-handed interfaces for electromagnetic surface waves. *Phys. Rev. Lett.* **98**, 073901 (2007).
- 8 Seddon, N. & Bearpark, T. Observation of the inverse Doppler effect. *Science* **302**, 1537-1540 (2003).
- 9 Hu, X. H., Hang, Z. H., Li, J. S., Zi, J. & Chan, C. T. Anomalous Doppler effects in phononic band gaps. *Phys. Rev. E* **73**, 015602 (2006).
- 10 Shi, S. Y., Chen, C. H. & Prather, D. W. Plane-wave expansion method for calculating band structure of photonic crystal slabs with perfectly matched layers. *J. Opt. Soc. Am. A* **21**, 1769-1775 (2004).
- 11 Notomi, M. Theory of light propagation in strongly modulated photonic crystals: Refractionlike behavior in the vicinity of the photonic band gap. *Phys. Rev. B* **62**, 10696-10705 (2000).
- 12 Martínez, A. & Martínez J. Negative refraction in two-dimensional photonic crystals: Role of lattice orientation and interface termination. *Phys. Rev. B* **71**, 1-12 (2005).
- 13 Foteinopoulou, S. & Soukoulis, C. M. Negative refraction and left-handed behavior in two-dimensional photonic crystals. *Phys. Rev. B* **67**, 2351071-2351075 (2003).
- 14 Feng, L., Lu, M. H., Lomakin, V. & Fainman, Y. Plasmonic photonic crystal with a complete band gap for surface plasmon polariton waves. *Appl. Phys. Lett.* **93**, 231105 (2008).
- 15 Johnson, S. G., Fan, S., Villeneuve, P. R., Joannopoulos, J. D. & Kolodziejcki, L. A. Guided modes in photonic crystal slabs. *Phys. Rev. B* **60**, 5751-5758 (1999).
- 16 Søndergaard, T., Bjarklev, A., Kristensen, M., Erland, J. & Broeng, J. Designing finite-height two-dimensional photonic crystal waveguides. *Appl. Phys. Lett.* **77**, 785-787 (2000).

Acknowledgements

This work is supported by the National Basic Research Program of China (2007CB935303, 2005CB724304), National Natural Science Foundation of China (60778031), and Shanghai Leading Academic Discipline Project (S30502). Min Gu acknowledges the support from the Australian Research Council (ARC) under the Centres of Excellence program and the Laureate Fellowship scheme (FL100100099). Baohua Jia thanks the ARC for the support through the APD grant DP0987006.

Statement of author contribution

J. C., S. Z. and T. G., designed and performed experiments, analysed data and wrote the paper; B. J., X. L. and M. G. designed the supplemental experiment and the physical strategy of numerical calculations, analysed data and wrote the paper; Y. W. and B. L., designed and performed experiments; L. F. and W. Q. performed experiments; X. Z. prepared the PC prisms.

Figure captions:

Fig. 1 **A schematic diagram showing Doppler effect. a**, Normal Doppler effect in normal materials ($n>0$). **b**, Inverse Doppler effect in negative index materials ($n<0$).

Fig. 2 **Experimental set up for detection of the inverse Doppler effect.** BS: beam splitter; ND: neutral density filter. The purple box highlights how the reference beam and the signal beam combine at the beam splitter.

Fig. 3 **Negative refractive index photonic crystal. a**, Scanning electron microscopic image of the 2D photonic crystals top view; Right inset: side view; left inset: geometry of the entire photonic crystal. **b**, Calculated band diagram of the photonic crystal. **c**, The equipfrequency surface contours of the PC at several relevant frequencies in the second band; **d**, The effective phase index n versus the frequency f for the second band along the ΓM direction.

Fig. 4 **Observation of inverse Doppler effect in negative refractive index photonic crystal.** **a**, Measured transmission power as a function of the refraction angle θ for a normally incident beam with respect to the first interface of the PC (the incident angle at the exit interface is 60°). Inset: Schematic diagram of the experimental setup. **b**, Measured frequency shifts Δf in the NIM PC prism compared with the value of $f'_2 - f_0 k$. Inset: Recorded signals with the PC prism at $v=0.0123 \text{ mm}\cdot\text{s}^{-1}$ ($\Delta f=0.89 \text{ Hz}$), $v=0.0245 \text{ mm}\cdot\text{s}^{-1}$ ($\Delta f=1.83 \text{ Hz}$), $v=0.0488 \text{ mm}\cdot\text{s}^{-1}$ ($\Delta f=3.65 \text{ Hz}$) and $v=0.0732 \text{ mm}\cdot\text{s}^{-1}$ ($\Delta f=5.14 \text{ Hz}$), respectively. **c**, Measured frequency shifts Δf in the positive index ZnSe prism compared with the value of $f'_2 - f_0 k$.

Fig. 1

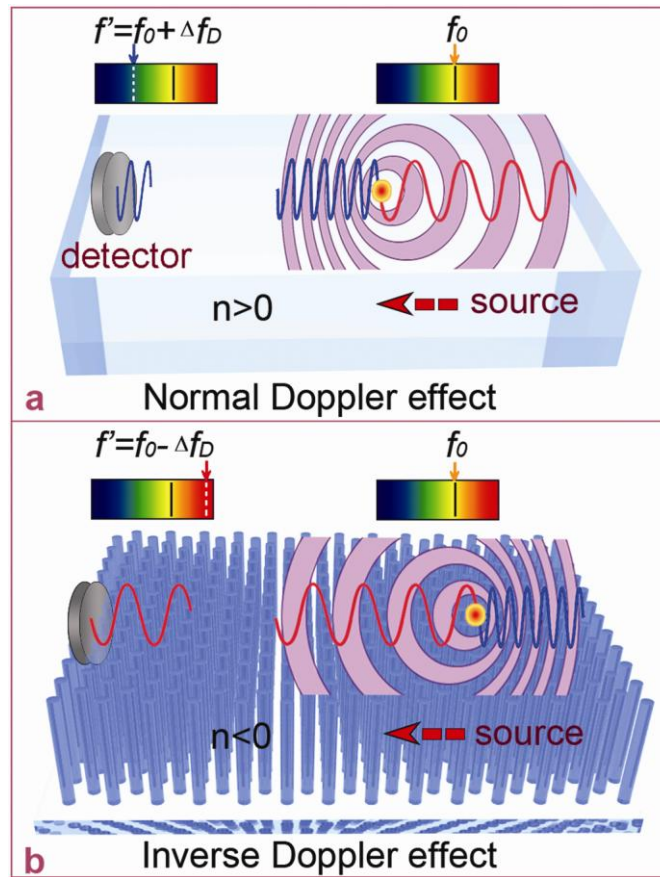


Fig. 2

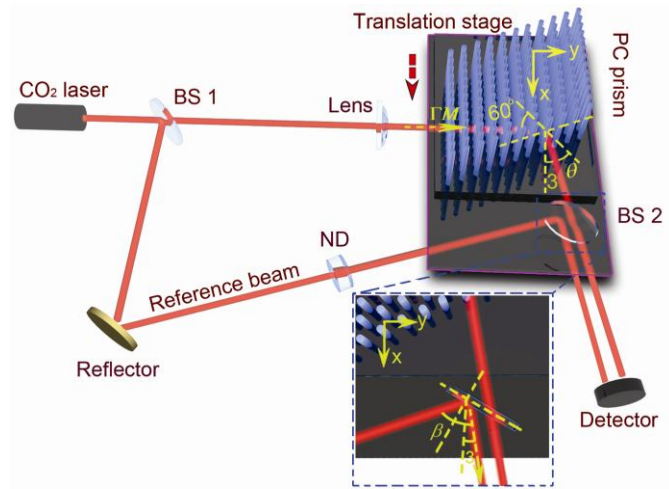


Fig. 3

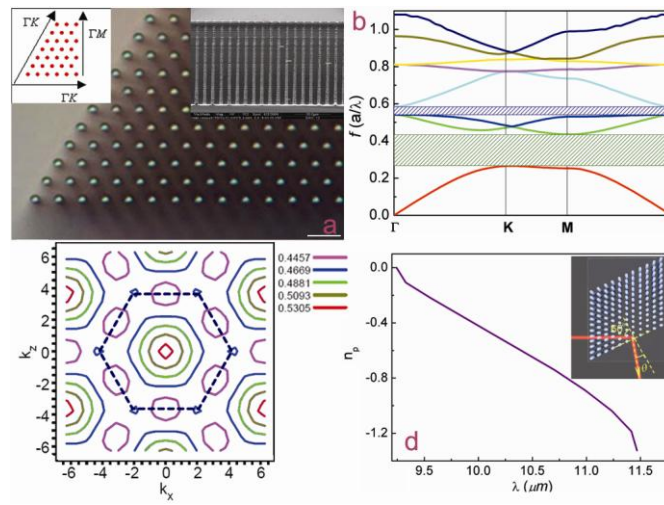


Fig. 4

